Comparison of carbon nanotube data using two microscopy methods: dark-field hyperspectral imaging and electron microscopy

A. Eastlake* and C. Geraci**

*National Institute for Occupational Safety and Health, Cincinnati, Ohio, aeastlake@cdc.gov
** National Institute for Occupational Safety and Health, Cincinnati, Ohio, cgeraci@cdc.gov

ABSTRACT

Analysis of electron microscopy samples can be quite costly and can take an extended period of time to complete, the National Institute for Occupational Safety and Health Nanotechnology research Center has been exploring the potential for using dark-field hyperspectral microscopy as a screening tool to identify nanomaterials. A pilot study has been performed where a given aerosol concentration of Mitsui multi-walled carbon nanotubes was loaded onto mixed cellulose ester filters using an acoustic aerosol generation system. These filters were then analyzed using both electron microcopy and dark-field microscopy. Microscopy samples were analyzed using modified NIOSH Manual of Analytical Methods 7402 and a counting convention proposed by NIOSH. Analysis of the data obtained in this study will provide much needed insight into the potential future use of this method to determine the count, identification, and concentration of nanomaterials on field-collected filter-based samples.

Keywords: dark-field hyperspectral microscopy, electron microscopy, carbon nanotubes, filter-based analysis

1 INTRODUCTION

Nanotechnology promises enhanced benefits to society by improving a wide variety of products and industries, including energy, medical, construction, coatings, materials, electronics, and optics. It is forecasted that the production volume of nanomaterials will reach over 6 million tons per year by 2020. (1) The unique nanoscale properties such as increased chemical reactivity, enhanced strength, thermal resistance, and electrical conductivity lend benefit to products that are being enhanced with nanomaterials. Surface reactivity and toxicological properties are affected as the particle size decreases and a greater proportion of surface area is available. This may lead to a difference in the biological activity as compared with larger particles of the same material. New technologies are often used prior to obtaining critical knowledge about worker, consumer, or environmental risk and nanomaterials are no exception. (2) The total number of nanotechnology workers is increasing annually, with estimates projecting 2 million workers in the United States and 6 million jobs worldwide by 2020. (3) Therefore, nanotechnology has the potential to play a significant role in the future of a variety of industries both within the United States and internationally.

Currently, the National Institute for Occupational Safety and Health (NIOSH) Nanotechnology Research Center (NTRC) uses a modified version of the NIOSH Manual of Analytical Methods (NMAM) 7402 (4) and electron microscopy (either scanning or transmission) on filter-based field samples to identify and confirm the presence, size, and degree of agglomeration of nanomaterials. Analysis of electron microscopy samples can be quite costly and can take an extended period of time to complete. The NTRC has been exploring the potential for using dark-field hyperspectral microscopy (HSI) to identify the presence and size of nanomaterials in air samples. This method has the potential for use as a “screening” method prior to or instead of electron microscopy.

NIOSH was first introduced to the potential for using HSI to view nanomaterials in 2009 at the Nanotech Conference & Expo (Houston, Texas). Subsequently, NIOSH purchased a Cytoviva® HSI system to support nanotoxicology research. Communication within the NTRC regarding the successes with detecting nanosized particles and fibers in tissue samples using the HSI system led to a proposal for a feasibility study to use HSI for the detection of nanoparticles from environmental samples. Without a definitive characterization of the sensitivity and specificity of the system, the focus of the feasibility study was targeted on the applicability of HSI as a screening and prioritization tool for nanoparticle air samples to be analyzed by electron microscopy. It is envisioned that a ruggedized method for air samples could be developed.

The HSI method makes use of an optical microscope that has been outfitted with a hyperspectral imaging system. This system can provide hyperspectral images to indicate the presence of nanomaterials in the visible near-infrared (VNIR 400nanometer (nm) -1,000nm) or in the short wave infrared (SWIR 900nm-1,700nm) wavelength ranges. All objects are identified based on confirmation of both visual pixels and the appropriate spectra. Total CNT counts, counts within specified CNT lengths, and fractional areas of CNT coverage can be obtained.

Although HSI has seen increased use in viewing nanomaterials in both *in vitro* and *in vivo* biological samples (5-9), there has been limited research performed in the evaluation of this method in filter-based nanomaterial samples. Due to the high cost and extended turnaround time for electron microscopy samples, the HSI method is being evaluated as a potential screening and prioritization tool

specifically for use in evaluating field-collected filter-based nanomaterial samples.

2 METHODS

A controlled specified aerosol concentration of Mitsui-7 multi-walled carbon nanotubes (MWCNTs) was created via an acoustic aerosol generation system (Figure 1). This system is able to sustain an aerosol concentration of 0.5 milligrams per cubic meter (mg/m^3). Mitsui-7 MWCNTs were used as they have been well characterized and used extensively in many NIOSH studies (7, 9-13). The filter-based samples were collected nominally at 4 LPM using Leland pumps (SKC Inc., Eighty Four, PA). Samples were collected on mixed cellulose ester (MCE) filters. Since the minimum sustainable concentration was 0.5 mg/m^3 and the flow rate was set at the maximum that the chamber would allow (4 LPM), the following filter exposure times were calculated for the specified loadings: 0.5 micrograms (µg) (exposure for 15 seconds), 1 µg (exposure for 30 seconds), and 3 µg (exposure for 90 seconds). Two filter sets were collected at each concentration.

Filter loading time was determined as the time that the filter was hooked up to the generation chamber. Loading concentrations were calculated based on the average concentration as determined by the sample generation DataRam and sample pump flow rate. A TSI model 3007 (TSI, Inc., Shoreview, MN) handheld condensation particle counter collected and data-logged particle count concentrations throughout the duration of the filter exposures to verify particle concentration.

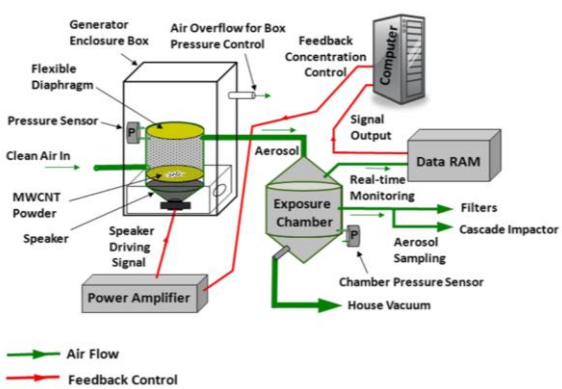

Figure 1. Diagram of acoustic generator and equipment set up used to expose MCE filters.

For HSI analysis, the MCE filters first had to be clarified. Filter holders were opened and the filter was removed under a vented hood. The filter was separated from its background support and placed with forceps on a clean surface. A 5 x 4 mm rectangular filter section was cut out and placed onto a precleaned glass slide. The edges of the filter were pressed to the glass to promote adhesion. A precleaned cover slip was carefully set so that one edge of the cover slip was approximately 2 mm from the membrane. Commercial grade acetone was applied to the edge of the cover slip in 20 µm amounts using a micropipette applicator. Acetone was applied six times to envelop the filter with a solvent bath to create an optically clear area. The size of the clarified area was approximately the same as the size of the original filter.

Images of clarified MCE filters were obtained under the optimized dark-field microscopy method, using HSI. In all cases, filters were imaged using a 40X air objective. The HSI scan covered an area of approximately 0.0005 centimeter^2, or approximately 0.01% of the full area of the membrane filter. This area is too small to provide a statistically conclusive MWCNT count so between four and six measurement scans were obtained for each MWCNT concentration. The spectral angle mapper (SAM) classifier tool was used to identify MWCNT in all images. SAM identifies image pixels containing MWCNT by matching the pixel spectrum with a library of spectra that were obtained from pixels known to contain MWCNT. The peak reflectance varied from 558 nm for the smaller, fainter MWCNT, to 610 nm for the larger, brighter MWCNT.

A set of digital binary filters were used to extract MWCNT objects from the classification images created by the SAM. The counting method assumes that single objects are defined by a connected set of pixels. Since it was possible for the SAM output to leave gaps in pixels that were found for each MWCNT object, a series of binary filters were applied to fill in gaps so that single objects were not counted more than once. A second binary filter produced "skeletonized" images of the MWCNT, of width equal to a single pixel, so that the pixel count translated into a length parameter. These methods were used to determine total number of MWCNT detected, total number of pixels containing a single-width MWCNT, mean length within specified range, and the fraction of the image covered by detected MWCNT.

In addition to the filters collected for HSI, filters were also collected for electron microscopy. Both transmission electron microscopy (TEM) and scanning electron microscopy (SEM) require analysis of bulk and blank samples in addition to filter-based samples. Analysis of the bulk sample allows the microscopist the opportunity to anticipate material appearance and characteristics. Blank filter-based and internal preparation process samples were analyzed to verify that the filters were not contaminated with materials that could interfere with the microscopic analysis.

Prior to TEM analysis, the filter samples were prepped using the NIOSH 7402 NMAM method with no etching. A minimum of two 3-mm copper grids were prepared for each filter and blank sample. The NMAM 7402 stopping rules for asbestos fibers analysis were applied to the carbon nanotubes. This requires the microscopist to view 40 grid openings or 100 structures in at least one grid opening. The following information was provided for each MWCNT sample: count and size, length and width, several representative images, and the presence of individual fibers, bundles, clusters or matrices present. The size of each

structure (whether individual or agglomerated) was determined. Samples were analyzed on a Philips CM-12 (FEI/Phillips, Hillsboro, OR). Two grids from each sample were examined at low magnification to determine the loading and preparation quality. Single or multiple grid openings from each TEM grid were examined unless 100 structures were counted in one opening.

Preparation of filter samples differed for SEM analysis. A portion of each filter was cut, placed onto carbon taped stubs and gold coated. The samples were then analyzed by a Tescan (Tescan, Czech Republic) scanning electron microscope (SEM) equipped with a Gresham light element detector and an IXRF digital imaging system (EDS). The microscopist visually moves across the filter at an even interval until a total particle count of 100, or a total screen count of 100 structures, are counted.

3 RESULTS

Due to the high cost of electron micrscopy analysis, many facilities may not confirm the presence of nanomaterials in air samples using electron microscopy. In addition to the mass based analysis for carbon nanotubes, it is important to visually confirm the presence of the nanomaterial.This can provide insight as to the presence, size, shape, potential for agglomeration, approximate quantity, and migration of the nanomaterial. In addition, visual confirmation of the naomaterial can indicate whether there is a need for and/or the efficacy of existing engineering controls and ventilation systems.

Electron microscopy (SEM and TEM) and HSI analysis of the MCE filters confirmed the presence of the Mitsui-7 MWCNTs (Figures 2 and 3). In addition, these images provide visual confirmation of the size, shape, and agglomeration potential of the MWCNTs. Confirmation of the expected material is perfomed using EDS for both SEM and TEM. HSI confirms the material by comparison of the pixel spectra with the spectral library. Each material provides its own spectral "fingerprint" which can then be used to identify the nanomaterial (Figure 4). All filters collected in this study, with the exception of blanks, indicated the presence of the loaded MWCNTs.

When HSI structure count per filter results (Figure 5) were averaged over the scans from all samples, the trend showed an approximate linear relationship between loading concentration and CNT count (R^2 = 0.9979). The best linear fit to the data points from pooled data, with the slope and the intercept shown is indicated in Figure 6. This corresponds well with the linear relationship achieved using electron microscopy (SEM R^2= 0.9848 and TEM R^2=0.9761).

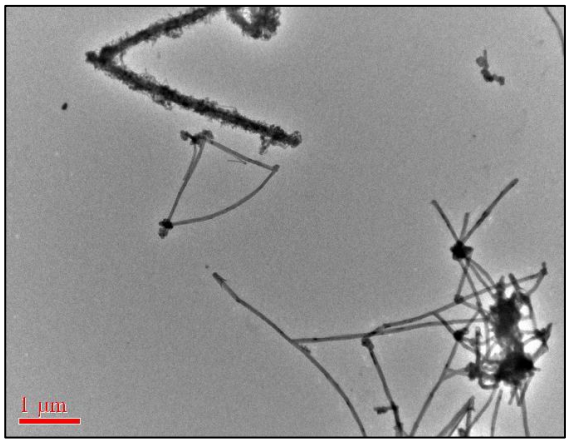

Figure 2. TEM image of MWCNTs at 3.0 µg filter loading concentration.

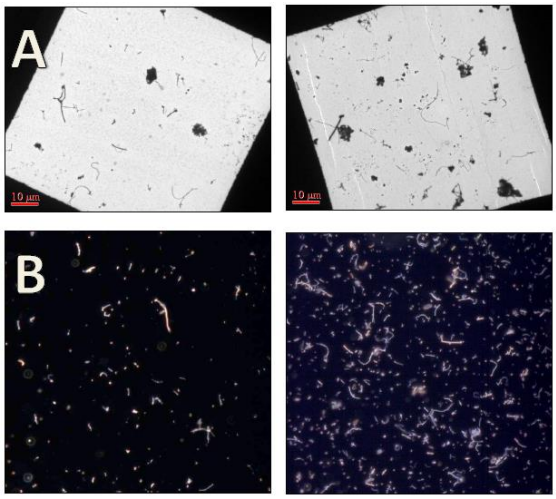

Figure 3. Images of MWCNTs at two different concentrations. Left: 1.0 µg. Right: 3.0 µg.
A) TEM B) HSI

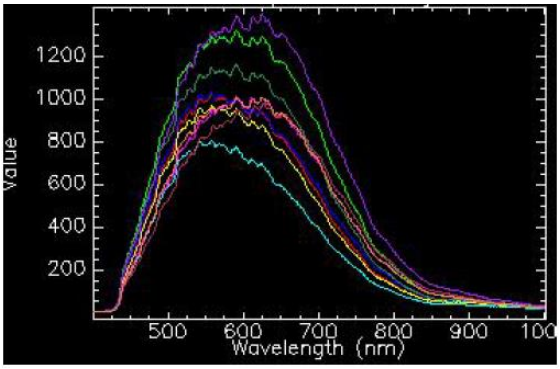

Figure 4. Example of HSI spectral library data used to classify pixels from MCE filter samples.

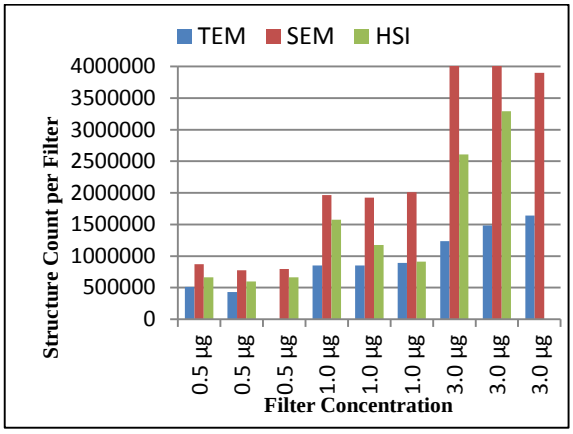

Figure 5. Structure Count per filter at three different MWCNT loading concentrations.
Results from dark-field HIS, TEM, and SEM.

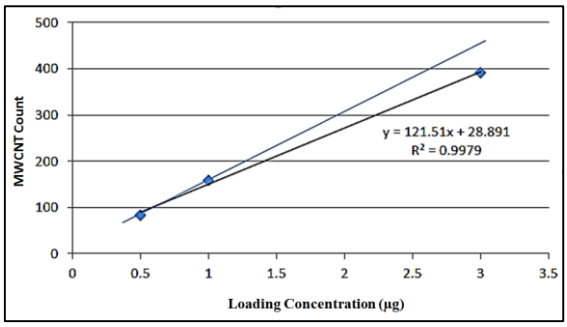

Figure 6. Linear relationship between filter loading concentration and MWCNT count using HSI.

4 CONCLUSIONS

This pilot study shows great promise for the use of HSI as a screening technique to determine the count, identification, and concentration of MWCNTs on a filter-based sample. As HSI is an automated proces, it is anticipated that this method could be used to decrease analytical time and manpower by preliminarily scanning filters to determine which filters would be most beneficial for analysis via electron microscopy analysis. Due to the small sample size and short exposure times, NIOSH has elected to repeat this pilot project to provide a larger sample number to further determine if this method will provide consistent results over multiple samples. The same sampling protocol will be followed and the same material will be used.

DISCLAIMER

The findings and conclusions in this report are those of the authors and do not necessarily represent the official position of NIOSH. The use of instrumentation and equipment by NIOSH does not constitute endorsement.

REFERENCES

1. Markets. F. The Global Nanotechnology and Nanomaterials Industry. Future Markets, Inc., 2012.
2. Howard J MV. National Nanotechnology Partnership to Protect Workers. Journal of Nanoparticle Research. 2009;11(7):1673-83.
3. Mihail C MA, Hersam M. Nanotechnology research directions for societal needs in 2020:retrospective and outlook. World Technology Evaluation Center (WTEC) Panel Report, National Science Foundation. 2010.
4. NIOSH. Method 7402. Asbestos by TEM. NIOSH Manual of Analytical Methods (NMAM). Baron PA, editor. Cincinnati, Ohio: United States: Department of Health and Human Services and Centers for Disease Control and Prevention; 1994.
5. Grabinski C, Schlager J, Hussain S. Hyperspectral microscopy for characterization of gold nanoparticles in biological media and cells for toxicity assessment. Nanomaterial Interfaces in Biology: Springer; 2013. p. 167-78.
6. Wang L, Castranova V, Mishra A, Chen B, Mercer RR, Schwegler-Berry D, et al. Dispersion of single-walled carbon nanotubes by a natural lung surfactant for pulmonary in vitro and in vivo toxicity studies. Particle and fibre toxicology. 2010;7(1):31.
7. Mercer RR, Hubbs AF, Scabilloni JF, Wang L, Battelli LA, Friend S, et al. Pulmonary fibrotic response to aspiration of multi-walled carbon nanotubes. Particle and fibre toxicology. 2011;8(1):21.
8. Stacy BM, Comfort KK, Comfort DA, Hussain SM. In Vitro Identification of Gold Nanorods through Hyperspectral Imaging. Plasmonics. 2013;8(2):1235-40.
9. Porter DW, Wu N, Hubbs A, Mercer R, Funk K, Meng F, et al. Differential mouse pulmonary dose-and time course-responses to titanium dioxide nanospheres and nanobelts. Toxicological Sciences. 2012:kfs261.
10. Hubbs A CV, Chen BT, Frazer DG, McKinney W, Mercer RR, Kashon ML, Battelli LA, Willard P, Porter DW., editor Pulmonary inflammation, epithelial hyperplasia, and lymph node translocation after multi-walled carbon nanotube inhalation. The Toxicologist Society of Toxicology 50th Annual Meeting and ToxExpo 2011; Washington, DC.
11. Birch ME, Ruda-Eberenz TA, Chai M, Andrews R, Hatfield RL. Properties that influence the specific surface areas of carbon nanotubes and nanofibers. Annals of occupational hygiene. 2013;57(9):1148-66.
12. Mercer RR, Hubbs AF, Scabilloni JF, Wang L, Battelli LA, Schwegler-Berry D, et al. Distribution and persistence of pleural penetrations by multi-walled carbon nanotubes. Particle and fibre toxicology. 2010;7(28):1-11.
13. Erdely A, Dahm M, Chen BT, Zeidler-Erdely PC, Fernback JE, Birch ME, et al. Carbon nanotube dosimetry: from workplace exposure assessment to inhalation toxicology. Particle and fibre toxicology. 2013;10(1):53.